



Cascaded Multilevel PV Inverter with Improved Harmonic Performance during Power Imbalance between Power Cells and reduced the switches

K. Mohan¹, Dr G. Seshadri²

1 PG Scholar, Dept of EEE, Narsimha Reddy Engineering College, Hyderabad, TS, India

2 Counselor, Dept of EEE, Narsimha Reddy Engineering College, Hyderabad, TS, India

Abstract: In a cascade multilevel converter, the difference in power cell illumination causes the duty cycle to vary between these cells while maintaining Maximum Power Point Tracking (MPPT). However, the cell duty cycle difference is undesirable because it is corresponding to the result voltage and current mutilation. In such manner, staggered geographies for photovoltaic (PV) applications using H6 bridge power cells instead of H-bridge cells are proposed. If there is a solar mismatch between the power cells, the proposed converter will power the shaded cells at a lower voltage without changing the voltage of the solar module. So it continues to run MPPT. This modification ensures that all power cells maintain the same cycle of work in any weather conditions. Therefore, it maintains excellent Output voltage and current characteristics. To test the viability of the proposed arrangement, detailed simulation models and test prototypes were constructed. They got results show that the proposed geography gives fundamentally worked on output voltage and current characteristics compared to the cascaded H-bridge. The performance of the proposed topologies is also compared with the topology providing improved harmonic performance according to European efficiency, with a recorded improvement of 2.64%.

Index Terms —Cascaded converter, Grid connected, H-bridge, MMC, MPPT, Partial shading, Photovoltaic, P&O, Power quality.

I. INTRODUCTION

Multilevel (MLCs) are surprisingly reliable candidates for energy conversion appealing features and do not respond well [1] [3]. These electro-geological converter circuits are capable of generating first-order Voltage waveform with power switch working even at the central recurrence when the level count is sufficiently high. Then again, the high voltage permits the utilization of result channels of less power [4]. The cascaded H-Bridge converter topography [5] with a serial H-Bridge interface, all handled by an alternate DC voltage source? This brand name allows you to connect PV sheets on each H-interface. An unprecedented follow-up power is then reached to process the power of the entire structure and collect the energy is included in [6]. A usually utilized PWM strategy in MLC is PSPWM [7]. PSPWM in CHB use is portrayed as a multi-carrier, one is doled out to each H-bridge, where these transporters move T_s/n comparative with each other. Where T_s is the carrier commitment period and n is the amount of H-ranges. A comparable power scattering and comparable energy catastrophe between shock cells is

suggested when using this recommended system, and a multiplier effect (2 nmf) appears when repeating the converter's output voltage change [7]. In any case, the design will be distorted if the strength element is exposed to disproportionately large insolation due to build-up or primarily masking compared to the PV sheet. These imbalances can be classified into two classes: anomalies in the covering phase and volume in the burial phase. The past is perceived as an outdated problem, reminiscent of the question of clumsiness at the burial stage with many plans in the essay [8]. Taking all this into account, a new operating mode is introduced in which a staggered transducer is applied [9], [10]. In any case, the one-sided problem of the cover is a modern problem caused by testing on cascading converters. An important driving force behind the sound transmitted by an output converter when sunlight is incomparable to a power cell is the difference between the cell holding period and the dc associate voltage. A cycle long enough in the indoor electricity mobileular to suit the brand new MPP modern as daytime decreases. So the modulator gets every other latch cycle. In this case, the hidden electricity mobileular

begins off evolved energizing with a selected delay (TD) and forestalls injecting earlier than the predicted TD time. However, in MLC, the tele cell smart phone is assembled to shape the output signal (output modern and voltage) of the converter, and the condition is a fundamental limit, i.e. the undeniable level or permissible movement of any power cell out of its intended position. May be violated Concession signal.

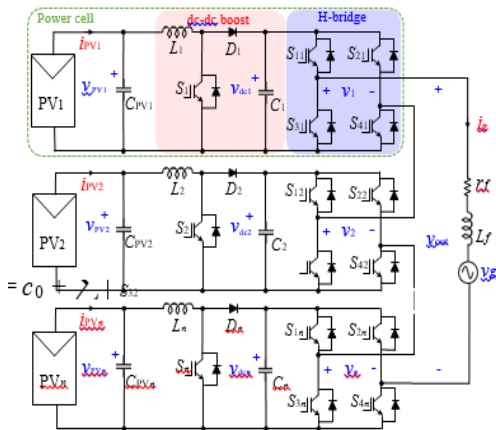


Fig. 1 The old style dc-dc boost H-bridge -primarily based totally electricity mobileular MLC (CHBB).

A infrequently any undertakings to lessen this trouble are represented with inside the composing [11]-[15]. In [11], a variable buying and selling focuses is the simple motion rule, in which this technique gives a humble plan; in any case, it's miles giant precisely while n=three in view of the amazing estimation required. Also, at some point of do away with halfway shadings, converting the service shift focuses doesn't in addition foster the yield alerts nice to an enough level. The makers in [12] proposed crafted via way of means of a further battery-handled electricity mobileular to triumph over this trouble if n=2. A dc-dc aid converter has been introduced into every electricity mobileular in [13], as proven in Fig. 1 (insinuated as CHBB from that factor on), in which a modified equilibrium framework is proposed to hold the strength some of the dc-accomplice capacitors at a close to level; on this manner, running all the cells at comparable dedication cycles. Specific fell staggered semi Z-supply inverter (sZSI) gives flexibility with inside the electricity nice count because the H-platforms' voltages are unfastened at the PV voltages—handiest more than one adjustments on its tenet and manage are required, as clarified in [14].

The motion of strong country transformer-primarily based totally electricity mobileular in a star-associated CHB inner seeing each interphase and intraphase disparity is moved in [15]. The as of overdue cited topography primarily based totally guides of motion integrate a number of dynamic and uninvolved additives—specifically inductors—with inside the electricity cells, and each so often, better buying and selling repeat is required, which now no longer really constructs the size, weight, and value of the converter, but likewise undermines the system's standard capability. In this paper, a H6 electricity mobileular-

primarily based totally Proposed MLC, where difficulty in discriminating dedication cycles is recognized. Note that this topic is an eruption from [16], which analyzes further speculation about the sounds introduced into the MLC on account of disproportionate power cells further as check impacts are presented.

The paper is facilitated because the going with, Section II examinations the fragmented disguising with inside the everyday CHB and the same old additives in the back of the yield voltage and contemporary turns below such case. Proposed region is given in Part III. Part IV suggests the management technique to be applied to run the proposed converter, since a trade-off is established for most switches. Part V analyzes tips and likes of overdue introduced guides of motion pointed into directing from the sounds content material at some point of commonly disguising. Reenactment and initial assessment exams are proven and inspected in part VI. Locale VII shuts the gave work.

II. EXAMINATION OF THE PARTIAL SHADING IN THE CONVENTIONAL CHB TOPOLOGY

A Fourier sweep is perhaps the most exemplary and fairly accurate device for signal preparation [17]. Therefore, in this article we will use it to analyze the output signal quality of the converter. According to Fourier's theory, any power $f(t)$, given the sum of sine and cosine, can be expressed as balancing dc as

$$f(t) = e_o + \sum_{h=1}^{\infty} [a_h \cos(h\omega t) + b_h \sin(h\omega t)] \text{--- (1)}$$

Where ω is the littlest precise recurrence to assess? The coefficients a_h and b_h are characterized as

$$\left. \begin{aligned} a_h &= \frac{1}{\pi} \int_0^{2\pi} f(t) \cos(h\omega t) d(h\omega t) \\ b_h &= \frac{1}{\pi} \int_0^{2\pi} f(t) \sin(h\omega t) d(h\omega t) \end{aligned} \right\} \text{---- (2)}$$

The capacitance being studied in this article is the result voltage of the converter, which is the amount of all power cell voltages. The result i-th power cell voltage is considered as a rectangular sequence of heartbeats with variable binding cycles and can be expressed as

$$V_i(t) = v_{dci} D_i \text{-----(3)}$$

Where $i=1 \dots n$

For example, D_i and V_{dci} individually represent the required period and the voltage of the source cell i . Then Fourier evolution of the yield stress of each force cell can be reported as

$$v_i(t) = c_{oi} + \sum_{h=1}^{\infty} [a_{hi} \cos(h\omega_c t) + b_{hi} \sin(h\omega_c t)] \text{--- (4)}$$

Where

ω_c is the transporter recursion. Understanding that the time start is chosen so that the capacitance $V_i(t)$ exhibits uniform uniformity, we can simplify the layout by setting b_{hi} to 0. Along this line, the Fourier coefficient can be found as

$$\left. \begin{aligned} c_{hi} &= \frac{1}{\pi} \int_0^{D_i\pi} v_i(t) d(\omega_c) = v_{dci} D_i \\ a_{hi} &= \frac{2}{\pi} \int_0^{D_i\pi} v_i(t) \cos(h\omega_c t) d(\omega_c t) = \frac{2v_{dci}}{h\pi} \sin(h\pi D_i) \end{aligned} \right\} \text{---(5)}$$

The result Fourier to i th power cell voltage increase development Then it could be rendered like this:

$$v_i(t) = v_{dci} D_i + \sum_{h=1}^{\infty} \frac{2v_{dci}}{h\pi} \sin(h\pi D_i) \cos(h\omega_c t) \text{--- (6)}$$

In this way, the all out yield voltage can be portrayed as

$$v_{out}(t) = \sum_{i=1}^n \left(v_{dci} D_i + \sum_{h=1}^{\infty} \frac{2v_{dci}}{h\pi} \sin(h\pi D_i) + \cos(h\omega_i t + \theta_i) \right) \text{--- (7)}$$

Where

θ_i –i-th moving point of the conveyor considered as

$$\theta_i = \frac{2\pi}{n} (i - 1) \text{--- (8)}$$

As shown in (7), the substance of the hth consonant at the most extreme result voltage is communicated as

$$v^k = \sum_{i=1}^n \frac{2v_{dci}}{h\pi} \sin(h\pi D_i) \cos(h\omega_c t + \theta_i) \text{--- (9)}$$

Assuming the converter has 3 energy elements, the harmonic content material h must be written as (10) below.

$$v^k = \frac{2v_{dc1}}{h\pi} \sin(h\pi D_1) \cos(h\omega_c t) + \frac{2v_{dc2}}{h\pi} \sin(h\pi D_2) \cos\left(h\omega_c t + \frac{2\pi}{3}\right) + \frac{2v_{dc3}}{h\pi} \sin(h\pi D_3) \cos\left(h\omega_c t + \frac{4\pi}{3}\right) \text{--- (10)}$$

In (10), for the h-th consonant material to bypass the full output voltage, the dc interface voltage and the required cycle must be equal. If semi-covered, management will scale back the covert unit's full deployment model so that flow is restricted to a lower level as indicated by the severity of the incomplete cover. An exemplary model was performed and presented in this article to further illustrate the results of numerical derivation on figs. Figure 2 shows the experiments for the coordinated and non-uniform KGB task. As should be visible from the (cz) chart here, the latch cycle is reduced because the third cell is hidden, so that the cell with a delayed TD starts to introduce energy and stops earlier than the expected time to TD. This reduction in binding cycle results in a few heartbeats being thinner or missing entirely from the overall output voltage, resulting in kinks in the last mentioned as shown in the zoom (see graph (dz)). It is also important to reduce the repetition of successful exchanges because there is no heartbeat, as shown in Figure 3. 2(d2).

III. PROPOSED MULTI-LAYER TOPOLOGY

As shown in (10), the choice to kill the h-th symphony material during semi-concealment is to equalize the period and tension of all telephones or extends all telephone appointment periods to approximate cohesion. Re-raise the hidden power cell-insertion model to a value close to adequate and uneven insolation between cells.

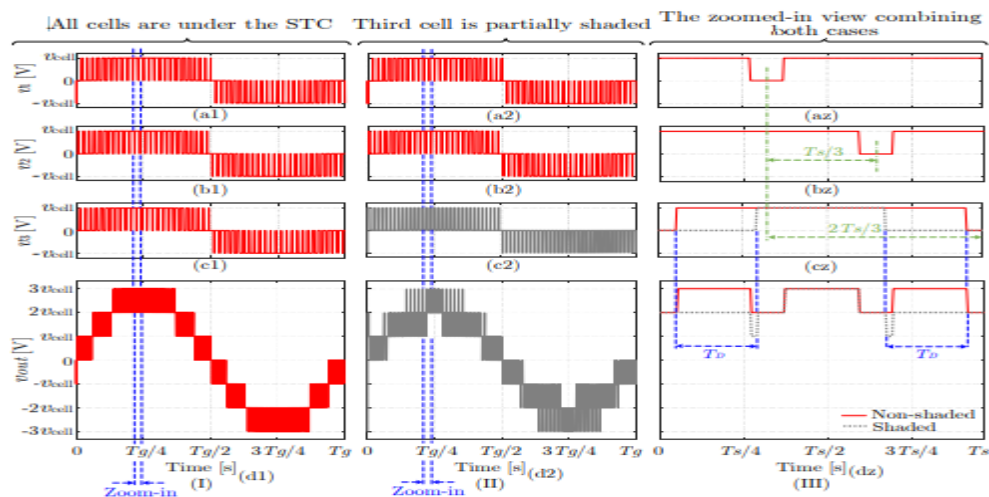


Fig. 2 The resulting voltage for all power cells case the came about absolute result voltage, in the two cases,

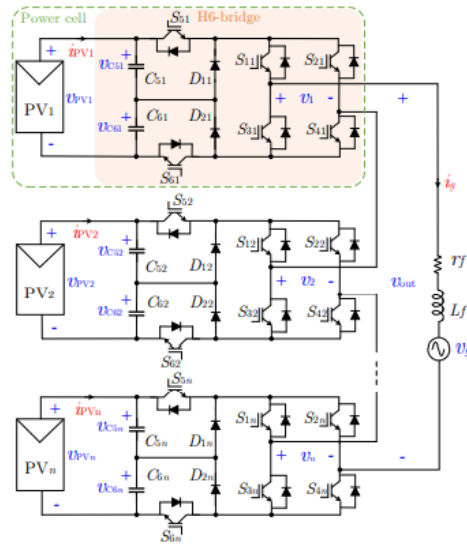


Fig. 3 Proposed Cascade Layer Topology for Solar System

Durability, the yield stress of the element must be reduced. In any case, the truth is not to change the voltage of PV and MPRT. A constant current stage can be utilized between every H-range and the PV strings to provide increased DC current and isolation voltage coupling between the PV strings. The DC/DC converter can be a lifting [13] (see fig. 1), a rotary brake [18] or a switch [19]. Nevertheless, this actuation interaction adds more inductor. Therefore, iron is more expensive and bulky. Also the dc-dc step is higher exchange cycles, conflictingly influencing the proficiency of the construction. Consequently, in this paper, we propose to displace the H-lady of the hour of each stage cell with H6. Here the DC interface capacitor is replaced by plug 1 and only 2 unique semiconductor tricks and 2 diodes are added. A typical layout of the proposed MLC for PV applications where n cells are considered is shown in Figure 1. The suggested idea is to supply power from a hidden power cell. A lower voltage without changing the voltage in the solar circuit (see Figure 4). So I keep the MPPT. The yield stress of each cell can be set as

$$v_i = (s_{1i} - s_{2i})(s_{5i}v_{c5i} + s_{6i}v_{c6i}) \text{--- (11)}$$

Where

Sxi is the dynamic state of semiconductor xi that can be turned on or off. As in the photo. 3 I am referencing a list of cells, where x is the number of semiconductors in that cell. The coefficients vi, vC5i and vC6i deal with the breakdown voltage, the capacitor C5 yield voltage of the ith cell, and the capacitor C6 yield voltage independently. In the event that the capacitor charge of each power cell is something very similar, the result voltage of the cell can be communicated as

$$v_i = v_{PVi}(s_{1i} - s_{2i}) \left(\frac{s_{5i} + s_{6i}}{2} \right) \text{--- (12)}$$

For example, vPVi is the voltage on the ith string terminal of the PV module. The specific conduct of every energy mobileular may be defined via way of means of an accompanying differential condition.

$$C_{\{5,6\}i} \frac{dv_{c\{5,6\}i}}{dt} = (i_{PVi} - (s_{1i} - s_{2i})s_{\{5,6\}i}i_g) \text{--- (13)}$$

Fig. 4 Activity state of the proposed power cell. Accordingly, as indicated by the Kirchhoff stress law, the general unique conduct of the casing can be assessed as (14)

$$L_f \frac{di_g}{dt} = \sum_{i=1}^n \left(s_{1i} - s_{2i} \left(\frac{s_{5i} + s_{6i}}{2} \right) v_{PVi} \right) - r_f i_g - v_g \text{--- (14)}$$

Where

ig, vg, Lf and rf are the framework current, cross section voltage, channel inductance and channel inside obstruction, only.

IV. CONTROL STRUCTURE OF THE PROPOSED TRANSDUCER

The board of directors of the proposed district is divided into three regions. Network current control, autonomous MPP, voltage guideline and control with capacitor H6 close to every cell. In this article, we utilize one corresponding regulator (PI) regulator for the voltage of One relative applicable (PR) regulator for each cell and output current to accomplish the past sort of control (see Figure 5) [6]. This control framework has demonstrated to be the best procedure while utilizing components with various voltages. This is on the grounds that these voltages are resolved utilizing a different MPP tracker [6]. As you can find in the photograph. 5, At $i=2$ to n , the cell voltage is a separately controlled component and is addressed by a circle. The voltage it is constrained by a PI regulator that sets the result signal.

V. COMPARISON OF THE RELEVANT PARTS AND THE PROPOSED TOPOLOGY

Table 1 is the proposed converters and geographic proposals that paintings for steady overall performance even as semi-hidden among phones, inclusive of debt, dynamic pressure Control of switches, switching frequency and complexity. As shown in this table, mobile power impedance sources (ICs) use inductors for every mobileular, while a CHBB energy mobileular makes use of one. However, the proposed converter does now no longer use it. For capacitors, IS energy cells once more the use of better values. Also, Power Cell IS. Utilize a few capacitors with incredible voltage rating that is similar to the whole mobileular voltage. The CHBB essentially based totally pressure mobileular makes use of comparable capacitors consist of as with inside the proposed geography; notwithstanding, one in all them paintings on the all out mobileular voltage. It has a tendency to be visible from Table I that the proposed geography makes use of the maximum noteworthy switches tally contrasted with its partners.

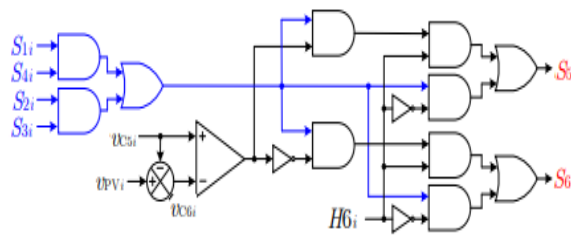


Fig. 4 Installing and balancing capacitors on partially shaded batteries

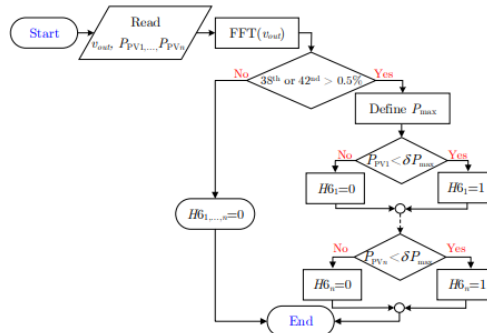


Fig. 5 Flowchart of Algorithm Used to Determine Partially Shaded Power Cells

By the way, the voltage to the key of the proposed H6 pad is a large proportion of the voltage in the other topologies during half-masking. It can be seen that the converter proposed in Table 1 operates at the lowest exchange rate, and BBB requires the most attention. Reduce rotation repetitions on uphill roads. However, this will be detrimental to the inductor size used. Because two inductors are used, the frequency of exchange in the power cell of the IS is lower than that of the BGV. However, all switches work at this recurrence, which is as yet higher than the proposed transducer. The next area will look at both exchange and conduction failures. Based on intrinsically safe power cells in sophistication, the MLC is amazing because the dual utility of the stage is converted into one and all inductor motions and capacitor voltages are constrained by comparative switches. CHBB is more straightforward to control in light of the fact that the voltage/current of the PV module is autonomously controlled by an auxiliary DC switch. The proposed geography is considered the most difficult to control. Because we can use the same control calculations we got for CHB. The only thing is to add a basic calculation to adjust the voltage across capacitors C5i and C6i, as seen in segment IV.

VI. SIMULATION RESULTS :

A. SYSTEM SPECIFICATIONS:

With the ultimate objective of pre-supporting the suggestion, organized and reshaped from PLECS as a 1 kW single stage inverter. The inverters planned have a voltage range of 120 to 190 V and consist of a solar string like the 2 mF capacitors in all phones. The boundaries of the solar board are taken from the original board passport of Alfasolar GmbH, model SI S21170.A1. This PV board has $v_{OC}=96V$, $v_{MPP}=76V$ data. $I_{SC}=2.83A$ and $i_{MPP}=2.2A$ under standard test conditions (STC). To accomplish an ideal voltage level following matrix bonding, two PV substrates were simulated connected in series to each cell with three cell counts. The network key size and repetition rate were set separately to $\sqrt{2}\times 230V$ and 50Hz, just like the neighbors. The H-spans exchange rate of all transducers tested was set to 2 kHz. The inductance of the output voltage channel was chosen to be 3.5 mH. The MPPT was a typical Irritate furthermore (P&O) type, with voltage lift and repeat set to 0.5V and 10Hz wholeheartedly.

B. TESTING PHASE:

The proposed converter was taken a stab at during the three time frames it came with. Initially, the platform starts running STC until MPPT is established, during which time switches S5i and S6i are turned on all the while to mimic CHB activity. Prior to the furthest limit of this stage, at the 3.5 second time of the test, the transducer detects an unexpected drop in insolation by 1.5 seconds in the third cell and considers this a second time delay. During the second time span, switches S5i and S6i are as yet turned on all the while, mimicking CHB activity. During the 5 seconds of the test, the third power cell was at this point concealed, yet the edge began functioning as a savage inverter H6 with the semiconductor switches S5i and S6i starting normal operation as described in the previous section IV on figs. 7 shows three recently depicted time spans where power is considered decoupled from solar string and cell voltages. Note the force lines in the first and second cells in Figure 1. 7(a) is unsatisfactory because it harmonizes with the line of the main power cell.

Simulation diagram

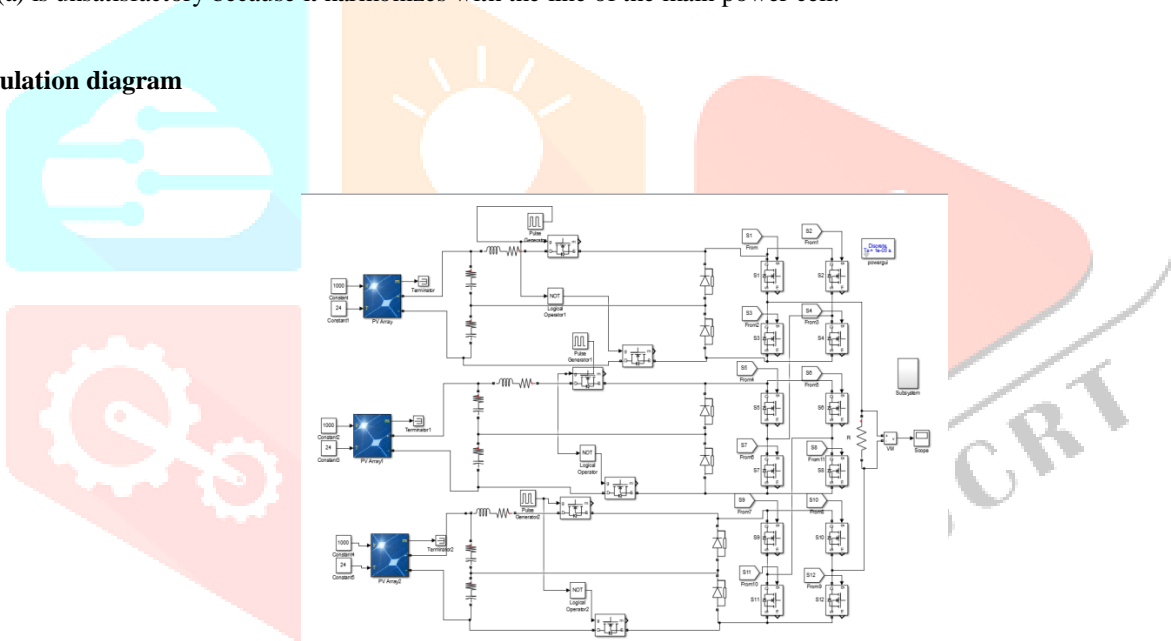


Fig. 6 Simulation model

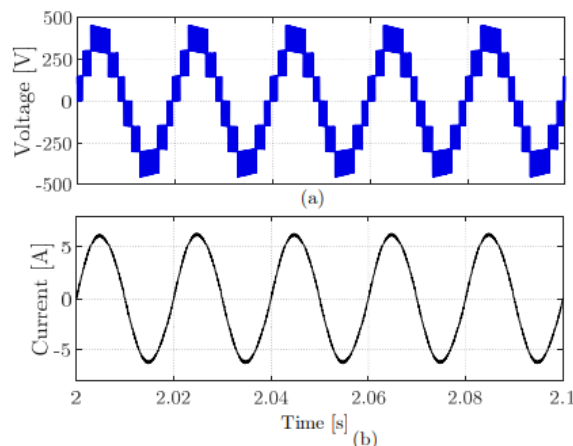


Fig. 7 (a) The outcome voltage, (b) the affiliation current, when the three PV strings of the proposed topography are under the standard test conditions

VIII. CONCLUSION

The critical explanations for the yield in this paper, we consider the current and voltage bending of the falling MLC, taking into account the imperfect protection between the strain cells. Of course, any differences in mobile bond cycles were identified as stress is the main factor distorting these yield signals. Also, if the mobile commitment cycle is nearly constant, the difference in mobile voltage should have a much smaller impact on this issue. Therefore, sham MLC was proposed. can offer tons much less voltage than the all out mobileular one, which, thus, permits the mobileular obligation cycle to be raised back to harmony after it diminishes if there should be an occurrence of halfway concealing. The proposition is practical, lighter, and less sizable since it doesn't need additional detached components regarding its partners. Just add dynamic segments. The proposed converter has been tried during reproduction and testing and has been shown to provide fully developed characteristics of the output voltage and current with fractional masking. Here TCHD is remembered according to the order of Symphony No. 50. For EN50160 standard, the voltage has been reduced from 15.23% to 10.75%.

IX. REFERENCES

- [1] F. Rong, X. Gong, and S. Huang, "A New Grid-Connected PV System Based on MMC to Maximize Power in Partial Shading," *IEEE Trans. Force Electron.*, vol. 32, no. 6, pp. 43204333, June 2017.
- [2] G. Farivar, B. Khredzak and V. G. Agelidis, "Sensorless Cascaded Multilevel Photovoltaic Systems Based on H-Bridge DC Side Transducers", *IEEE Trans. Industrial Electronics*, vol.1, p. 63, no. 7, pp. 42334241, July 2016.
- [3] Yu. Yu., G. Constantinou, B. Chredzak and V. G. Agelidis, "Power Balancing of HBridge Cascading Multilevel Transducers for Large-Scale Photovoltaic Integration", *IEEE Trans. Force Electron.*, vol. 31, no. 1, pp. 292303, Jan 2016
- [4] A. Lashab, D. Sera, J. Martins and JM Guerrero, "Cascaded DC Converter-Based Photovoltaic Systems with Integrated Energy Storage", 5th International Symposium on Clean Energy and Applications (EFEA), 2018, Rome, 2018 , p. 16.
- [5] Yu.Yu., Constantinou G., Grejak B., V. G. Ageldis, "Activity of Cascaded Multi-Level HBridge Converters for Large-Scale Solar Power Plants in the Event of Bridge Failure", *IEEE Trans. Industrial Electronics.*, vol. 62, no. 11, p. 72287236, August 11, 2015.
- [6] E. Villanueva, P. Correa, J. Rodriguez and M. Pacas, "HBridge Single-Phase Cascading Multi-Level Inverter Control for Grid-Connected Solar Systems," *IEEE Trans. Industrial Electronics.*, vol. 56, no. 11, pp. 43994406, Nov 2009
- [7] J. I. Leon, S. Curo, L. G. Frankelo, J. Rodriguez and B. Wu, "Basic Work and Continuous Development of Tuning Strategies for Current and Future Power Devices, for Voltage Source Inverters," *IEEE Trans. Industrial Electronics.*, vol. 63, no. 5, pp. 2688–2701, May 2016.
- [8] M. Honbu, Y. Matsuda, K. Miyazaki and Y. Jifuku, "Identical GTO Inverter Performance Techniques for Large AC Motor Drives", *IEEE Trans. Industrial Applications.*, vol.1, p. IA19, no. 2, p. 198205, March 1983
- [9] H. D. Tufty, A. I. Maswood, G. Constantinou, C. D. Townsend, P. Akuna and J. Pou, "Adaptive Control of HBridge Cascade Converters Connected to PV Grids During Unbalanced Voltage Drops," *IEEE Trans. Industrial Electronics.*, vol. 65, no. 8, pp. 6229–6238, 2018.
- [10] B. Xiao, L. Hang, J. Mei, C. Riley, L. M. Tolbert and B. Ozpineci, "Particular Cascaded HBridge Multilevel PV Inverter With Distributed MPPT for GridConnected Applications," *IEEE Trans.Ind. Applications.*, vol. 1, p. 51, no. 2, p. 17221731, March 4, 2015.
- [11] A. Marquez, H.I. Leon, S. Vazquez, R. Portillo, L. G. Frankelo, E. Freire, S. Curo, "Variable Point Stage Shift PWM for Direct Connected Cascaded Three-element Converters", *IEEE Trans. industry E*, no. 64, no. 5, pp. 3619–3628, May 2017
- [12] A. Marquez, H.I. Leon, S. Vazquez, L. G. Frankelo and S. Kuro, "PVbattery Framework Crossover Activity in Progress Symphony Performance", *ICON 2017 43rd Anniversary. Conference IEEE Industrial Electronics. Soc.*, Pp. 4272–4277, 2017.
- [13] K. Wang, K. Zhang, J. Xiong, Y. Xue and W. Liu, "Efficient Modulation Strategies for Cascade PV Systems Suffering from Module Mismatch", *IEEE J. Emerg. sat. up. Force Electron.*, vol. 6, no. 2, pp. 941–954, 2018.
- [14] C. Wang, K. Zhang, L. Liu, W. Liu, "A record control method applied to a pv-drop-based promiscuous Zsource-based module," *ICON 2015 41st Annu. Conference IEEE Industrial Electronics. Society, Yokohama*, 2015, p. 004911004916.
- [15] F. V. Amaral, T. M. Parreiras, G. C. Lobato, A. A. P. Machado, I. A. Pires and B. de Jesus Cardoso Filho, "Activities of Cascaded Multilevel Grid-Connected Converters Based on Direct Solid State Transformers in Unbalanced Solar Power Generation", *IEEE Trans. Industry Annex, Volume 1*, p. 54, no. 5, pp. 54935503, September, October 2018